

Portland State University

PDXScholar

Mechanical and Materials Engineering Faculty
Publications and Presentations

Mechanical and Materials Engineering

5-15-2018

Ozone Removal Efficiency and Surface Analysis of Green and White Roof HVAC Filters

Omed A. Abbass

Portland State University

David Sailor

Arizona State University

Elliott Gall

Portland State University, elliott.gall@pdx.edu

Follow this and additional works at: https://pdxscholar.library.pdx.edu/mengin_fac



Part of the [Materials Science and Engineering Commons](#), and the [Mechanical Engineering Commons](#)

Let us know how access to this document benefits you.

Citation Details

Abbass, O. A., Sailor, D. J., & Gall, E. T. (2018). Ozone removal efficiency and surface analysis of green and white roof HVAC filters. *Building and Environment*, 136, 118-127.

This Post-Print is brought to you for free and open access. It has been accepted for inclusion in Mechanical and Materials Engineering Faculty Publications and Presentations by an authorized administrator of PDXScholar. For more information, please contact pdxscholar@pdx.edu.

Ozone removal efficiency and surface analysis of green and white roof HVAC filters

Omed A. Abbass^{1,2}, David J. Sailor³, and Elliott T. Gall¹

1. Portland State University, Portland OR, USA; 2. University of Kirkuk, Kirkuk, Iraq; 3. Arizona State University, Tempe, AZ, USA

ABSTRACT:

Heating, ventilation, and air-conditioning (HVAC) system filters from a commercial building were tested for their ability to remove ozone from intake air. Filters were taken from rooftop HVAC systems installed for two months: one located on a white membrane roof and the other on a vegetated green roof. One new, unused filter sample was tested as a reference. Samples from these filters were exposed to ozonated air streams at 40 and 120 ppb and relative humidity levels of 30% and 70%. Filter surfaces were analyzed with a scanning electron microscope to observe the structure and composition of the materials loaded on each filter before and after exposure to ozone. The results show that for all samples tested, the ozone removal efficiency decreases with continued O₃ exposure. Removal efficiencies of 5-15% for white roof and unused filter samples, and 10-25% for green roof filter samples were observed after 5 hours of exposure to O₃. Filters taken from HVAC units located in the green roof area showed more ozone removal than unused filters or those taken from white membrane roof area. Unexpectedly, the unused filter samples had slightly higher ozone removal than the white roof filter. The data also show that the ozone removal percentage is higher when tested with 40 ppb ozone inlet concentration than at 120 ppb. SEM images show deposits of biotic material that are present on green roof samples, ostensibly explaining the greater ozone removal efficiency of filters from vegetated roofs.

Keywords: HVAC filters, ozone, green roof, ozone removal.

1. INTRODUCTION

The heating, ventilation, and air-conditioning (HVAC) system is central to ensuring the comfort and health of occupants of built environments. In commercial buildings, an HVAC system modulates the temperature, relative humidity, and levels of air pollutants in the indoor space via a combination of recirculation, filtration, and outdoor air ventilation. The intended role of an HVAC filter in a ventilation system is to trap particulate matter in the air supply system, for the protection of both occupants and downstream HVAC equipment. However, some research suggests that HVAC filters contribute to the removal of other air pollutants, including ozone (Zhao et. al. 2007). Ground level ozone is a contaminant that forms outdoors as a result of a photochemical reaction between nitrogen oxides (NO_x) and volatile organic compounds (VOCs) in the presence of sunlight (Pudasainee 2006). Ozone is an oxidant gas that has adverse effects on human health, including contributing to acute mortality (Gryparis et al. 2004) and lung function disorders (Lippmann 1989). The US EPA National Ambient Air Quality Standard for ozone is 70 ppb averaged for eight hours (EPA 2015). However, much higher levels, in exceedance of 100 ppb, especially in summer, are observed in many cities (Davis and Speckman 1999, Taha and Sailor 2010, Shao et. al 2009).

Outdoor ozone is transported indoors through the ventilation system and via infiltration across the building envelope. Outdoor ozone is removed by buildings through reactions with the building envelope (Stephens et al. 2011; Lai et al. 2015), HVAC system components like ducts and filters (Morrison et al. 1998), and interior surfaces (Abbass et al., 2017; Rim et al., 2016). Some HVAC filters are made of fibers with carbon-containing compounds, which may provide surface reaction sites where ozone chemistry can occur (Yang et al. 2017). However, the removal efficiency of unused filters is generally low for filters not specifically targeting ozone (e.g.,

Shields et al. 1999; Weschler et. al. 1994). For instance, Zhao et. al. (2007) compared ozone removal of filters made from synthetic fiberglass materials that were either unused or used in residential or commercial buildings. The results show low ozone removal values of 0 to 9% for unused filters and values ranging between 10 and 41% for used filters. Lee and Davidson (1999) tested the ozone removal efficiency of ten commercial filters that include granular activated carbon in their composition. The test results show that ozone removal efficiency of activated carbon filters varied over a broad range, from 4.6% to 98% based on filter type. These results imply filter composition can substantially affect O₃ levels in ventilation air.

While ozone removal is beneficial, reaction products may form due to ozone chemistry on filters. For instance, Lin and Chen (2014) have studied ozone removal and carbonyl generation from HVAC filters taken from different buildings; their results show low ozone removal percentage (less than 10%) for non-activated carbon containing filters. However, for used filters, ozone removal ranged between 10-92%. Carbonyl concentrations resulting from ozone reactions with filters or material deposited on filters ranged between 2-20 µg m⁻³ except for the tested activated carbon filter, which was ~90 µg m⁻³. Hyttinen et. al. (2006) conducted a study of ozone removal and VOC emissions from dusty, clean, and sooty filters taken from different buildings with variable deployment time. The effect of dust load, diesel soot, relative humidity and time of exposure were studied. Samples were tested in a small laboratory scale test apparatus with inlet ozone concentration ranged from 22 – 77 ppb. The results show differences in ozone removal among filter types where no ozone removal was observed from unused polyester filters, and higher ozone removal (25-30%) with higher TVOC emissions from in soot loaded filters. From these studies, it is clear that the loading of HVAC filters impacts both ozone removal and byproduct formation, with consequences for indoor air quality.

Many commercial HVAC units are installed on rooftops of building; rooftop HVAC consume substantial energy while affecting indoor air quality (Zaatari et al. 2014). At the same time, two increasingly popular building practices impact the nature of the rooftop surface: green roofs and white membrane roofs. Green roofs, also known as ecoroofs or vegetated roofs, are roofs containing a substrate layer that serves as a medium for growing plants (Sailor 2008). It has been suggested that green roofs increase building energy-efficiency, improve storm water management, and reduce the urban heat island effect (Berardi et. al. 2014), although outcomes vary as a function of specific design criteria like extent of vegetative cover (Sailor et al. 2012). White membrane roofs are covered with a thin white membrane layer to increase albedo that contributes to reductions in roof surface temperature, increasing building thermal efficiency and mitigating the urban heat island effect (Oleson et. al. 2010; Coutts et al. 2013). Given that outdoor ventilation air intakes are frequently sited on building rooftops, it is possible that the nature of the rooftop surface immediately surrounding the ventilation air intake impacts the quality of air entering the HVAC system. This may be due to fluxes of gases (Carslaw et al. 2015)) and/or re-suspended particles (Massey et al. 2012) from the rooftop that are transported into the HVAC system by wind or heat induced vertical mixing.

The objective of this research is to investigate the ozone removal efficiency of HVAC filters installed in air handling units located on green and white roof areas of a single commercial building and to compare results to a new, unused filter. We propose that the differences in fluxes of gas and/or particle-phase pollutants from either vegetated or white membrane roofing materials affects the amount and type of HVAC filter loading, in turn impacting ozone removal by HVAC filters. We apply scanning electron microscopy (SEM) imaging and chemical analysis to analyze the surface deposit composition of new and used filters, pre and post-ozonation. These

data provide insights as to the mechanisms by which filter fouling, ozone removal, and byproduct formation are related in filters taken from a location with two increasingly common roofing types.

2. METHODOLOGY

2.1 MATERIALS:

In this research, three identical HVAC filters (Purolator, CLARCOR Air Filtration Products, Inc.) with dimensions of 24"x24"x2" (609 mm x 609 mm x 50 mm) with a high capacity MERV 8 rating were used in tests. Filters were made of a mixture of polyester and polyolefin fabric as confirmed by the manufacturer. Two filters were taken from air handling units situated in green roof and white roof sections of a commercial building in Portland, Oregon, USA. Each filter had been installed and in service on the rooftop for a period of two months (September-October, 2015). The test field site is further described in Section 2.2. A new, unused filter was also tested to both evaluate ozone removal to unused filters and to provide a reference for comparison of SEM images and ozone removal by used filters. All filters were sampled from the field, wrapped with aluminum foil and stored in the original packaging in a controlled laboratory environment until they were tested for ozone removal, SEM imaging, and chemical composition.

2.2 FIELD SITE

Figures 1 and 2 show images, and a plan view for the site depicting both green and white membrane roofs. The roof of the building includes three extensive green roof sections with total area of 3600 m² adjacent to a white membrane roof with area of 5486 m². The green roof surface was covered with a vegetation layer composed of a mixture of succulents including several

species in the Sedum genus. The other section of the roof is covered with a conventional, waterproof white membrane. One air-handling unit is located on each roof from which air filters were sampled. The green roof air handling unit (AHU) is located at the center of green roof. The white membrane AHU is located near the center of white membrane roof as shown in Figure 1.

Figure 1. Plan view for the roof of the commercial building. The green section shows the green roof, and the white section shows the white membrane roof. AHU1 and AHU2 refer to locations where filters are sampled.

The AHUs for filter sampling were chosen as they operate nearly continuously. Other, smaller rooftop units (shown numbered 1-18 in Figure 1) were considered, but we observed that they operated with low fractional run-time. The larger AHUs chosen for this study treated a mixture of outdoor air and building return air, introducing a possible confounder from potential differences in compounds present in return air from the two indoor zones served by each AHU. However, our discussions with building management and knowledge of the site lead us to believe that the impact is minimal as both AHUs treat zones of the big-box retail store that are similar in use in that they contain a wide range of consumer products for sale.

Figure 2. A photo showing the green roof (left) and white membrane roof (right). One air handling unit is shown on the left photo with filters in the process of replacement.

2.3 EXPERIMENTAL APPARATUS

A diagram for the experimental test apparatus is depicted in Figure 3. The system includes an air supply system that purifies and conditions air to a desired humidity level. Purifying filters and drying media (Indicating Drierite, W.A. Hammond Drierite Co. Ltd.) were used before an activated carbon filter to ensure air purity and to remove VOCs present in supply air. A glass impinger filled with distilled water and by-pass valve was used to control the relative humidity of the supply air. A 12-bit combined sensor (Onset HOBO, S-THB-M008) was used to monitor and record temperature and relative humidity of the supplied air using a data logger (Onset HOBO, H21-002). A mass flow controller (OMEGA, model FMA 5523) was used to regulate the flow rate of air entering a stable ultra-violet (UV) ozone generator (UVP, model SOG-2). The ozonated air then was fed to a custom-fabricated two-piece filter holder made of PTFE. Two UV portable photometric ozone analyzers (2B Technologies, model 106-L) were used to record the ozone concentrations in one-minute interval upstream and downstream the chamber with a stated accuracy of the greater of 1.5 ppb or 2% of the reading. All tubing, connections, and valves were PTFE or stainless steel to minimize their reactivity with ozone.

Figure 3. Schematic diagram of the experimental apparatus

2.4 TESTS OF OZONE REMOVAL EFFICENCY

Samples of HVAC filters were taken from unused filters and filters located in HVAC units within the green roof and white membrane roof sections. Flat, circular samples of HVAC filters with diameter of 100 mm were cut to fit in the filter holder. To create an airtight seal, a portion of the filter was compressed between the mating surfaces of the filter holder; the

effective filter area exposed to ozone during experiments was 45.3 cm². The filter sample was securely mounted in the filter holder using flexible Teflon gaskets.

Prior to conducting each ozone removal efficiency test, the filter holder was washed thoroughly with distilled water, dried with a heat gun, and then quenched under a 380 ppb ozone stream for two hours. A test of ozone removal to the empty filter holder showed very small (~1%) ozone consumption since PTFE is inert to ozone reactions (De Smedt et. al. 1999). Samples of air filters were tested for ozone removal efficiency under different inlet ozone and relative humidity conditions, summarized in Table 1. The ozone removal efficiency tests were performed by providing ozonated air at a flowrate of 3.0 ± 0.075 LPM. This flow rate resulted in a filter face velocity of 1.1 cm s⁻¹. This value is similar to the face velocity value of 1.3 cm s⁻¹ reported by Destailats et. al. (2011) and by Zaatari et al. (2014) in a field study of 15 rooftop unit HVAC systems. Two inlet ozone values, 40 and 120 ppb, which varied $\pm 2\%$ across tests, and two relative humidity values 30, and 70%, which also varied $\pm 2\%$, were chosen as supply air conditions to cover a wide range of ozone and relative humidity levels used in other studies (Lee and Davidson, 1999; Morrison et. al., 1998). The monitored values for laboratory temperature were in the range of $21 \pm 1^\circ\text{C}$.

Ozone removal efficiency through a filter sample is defined according to equation 4, as described by Zhao et al. (2007):

$$E = \left(1 - \frac{C_e}{C_i}\right) * 100 \quad (4)$$

where C_e and C_i are ozone concentrations (ppb) at the exit and inlet of filter, respectively.

Uncertainty analysis using propagation of error was performed with inlet and outlet ozone concentrations measured with 2% accuracy each. Removal efficiencies were calculated for each

test from upstream and downstream ozone concentrations recorded for a period of five hours. To facilitate comparison across environmental conditions studied, we report both time-series removal efficiency and the removal efficiency to each filter for the final 20 min of each 5 h experiment, referred to as the five hour ozone removal efficiency (E_{5h})

Table 1. Summary of experiments for testing of ozone removal to and surface composition of filter samples

Experiment ID*	Filter sample from#:	Face velocity (cm/s)	Test chamber temp. (°C)	Ozone level (ppb)	Relative humidity (%)	SEM% analysis
GR_LowO3_LowRH	Green roof HVAC system	1.1	21	40	30	
GR_LowO3_HighRH					70	
GR_HighO3_LowRH				120	30	
GR_HighO3_HighRH					70	yes
GR_NoO3		N/A	N/A	N/A	N/A	yes
WM_LowO3_LowRH	White membrane roof HVAC system	1.1	21	40	30	
WM_LowO3_HighRH					70	
WM_HighO3_LowRH				120	30	
WM_HighO3_HighRH					70	yes
WM_NoO3		N/A	N/A	N/A	N/A	yes
New_LowO3_LowRH	Unused filter	1.1	21	40	30	
New_LowO3_HighRH					70	
New_HighO3_LowRH				120	30	
New_HighO3_HighRH					70	yes
New_NoO3		N/A	N/A	N/A	N/A	yes

*Experiment ID is the combination of the origin of the HVAC filter (green roof, white membrane roof, or unused filter) with low (40 ppb) or high (120 ppb) ozone conditions and low (30%) or high (70%) RH condition.

A sample was cut from the HVAC filter of the indicated origin. A different sample was cut for each test.

%SEM = scanning electron microscopy. Different samples were prepared for every SEM analysis.

2.5 PHYSICAL AND CHEMICAL ANALYSIS OF FILTERS

Six filter samples were prepared for SEM analysis, as noted in Table 1. Three were non-ozonated filter samples, and three were samples exposed to ozone. One sample was from an unused filter, while the other two were HVAC filters from the green roof and the white membrane roof. Square pieces (20 mm by 20 mm) of filter samples were cut for testing in the SEM chamber. The non-ozonated samples were also cut from collected HVAC filters, and the same process of ozone exposure described in sections 2.3 and 2.4 was repeated in preparing the ozonated samples at 120 ppb and 70% RH for subsequent SEM analysis.

Surface composition and elemental analysis of filter samples used employed simultaneous high magnification imaging and elemental analysis. In these analyses, a variable pressure scanning electron microscope (SEM) (Zeiss, Sigma VP) with nitrogen gas chamber at 50 Pa was used to obtain surface images for each filter sample at 100, 500, 1000, and 5000 \times magnifications. These images provide information about the construction and physical structure of filter fibers and deposited material on the surfaces of different filters. For elemental analysis of certain locations of filters, including filter fibers as manufactured (i.e., unused filters) as well as deposits accumulated on filter fiber surfaces, energy dispersive spectroscopy (EDS) was performed using an analyzer (Oxford Instruments, Xmax 50mm) attached to the SEM. EDS minimum detection limit is 0.1% by weight with accuracy within $\pm 2\%$ by weight. The analysis of data was performed using Aztec V 3.1 software. This technology enables qualitative and quantitative characterization of the elements composing the materials of filter fibers and deposits. The elemental analysis was performed at two locations for each of the filter fiber and deposited materials, determined by visual analysis of the magnified samples, for every filter

examined. A total of 34 unique locations were specified and analyzed for all ozonated and non-ozonated filters.

3. RESULTS AND DISCUSSION

3.1 EXIT OZONE CONCENTRATIONS:

Figure 4 shows inlet and outlet ozone concentrations for green roof, white membrane roof and unused filter samples at inlet ozone concentrations of 40 and 120 ppb at 70% relative humidity. Both subfigures show that exit ozone concentrations for green roof filters are lower, especially at the beginning of the tests, than other filter types. Exit ozone concentration for the unused filter sample is slightly lower than the white membrane roof filter. In addition, exit ozone concentrations during tests of both unused and white membrane roof filters reach near steady-state values in much shorter time than the green roof samples in both 40 and 120 ppb tests. However, for 120 ppb test, all exit values for all filters appear to reach a steady state value of about 100 ppb after about 150 min. but for inlet ozone tests of 40 ppb, the difference in exit ozone concentration is still noticeable between the three filter types. Lower exit ozone values reflect greater ozone reactions with either or both of filter fiber material and deposits on filters (Bekö et. al. 2007a). This reaction will consume some ozone, leading to lower concentration downstream of filters.

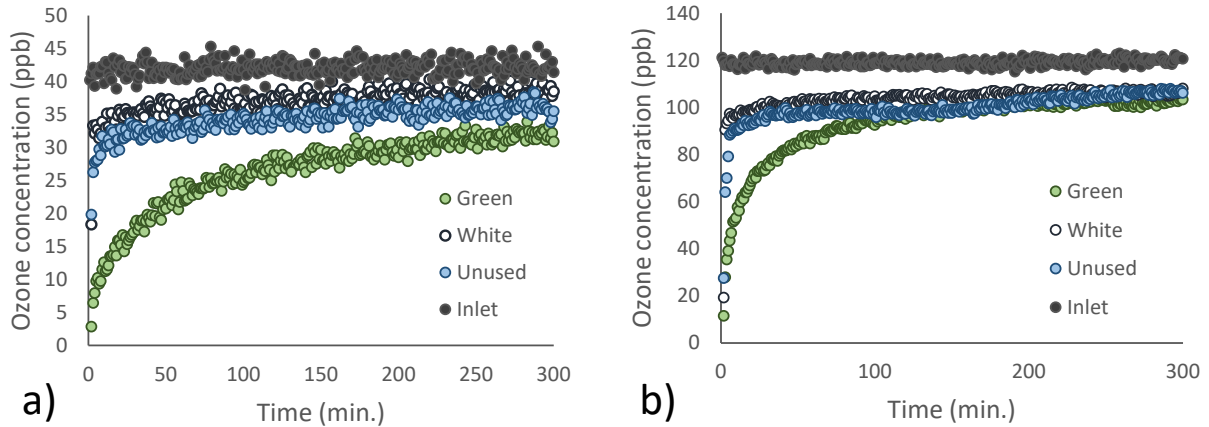


Figure 4. Inlet and exit ozone concentrations for green, white membrane roof, and unused filter samples. a) at 40 ppb ozone inlet. b) at 120 ppb ozone inlet. All tests performed at 70% RH inlet.

3.2 OZONE REMOVAL EFFICIENCY

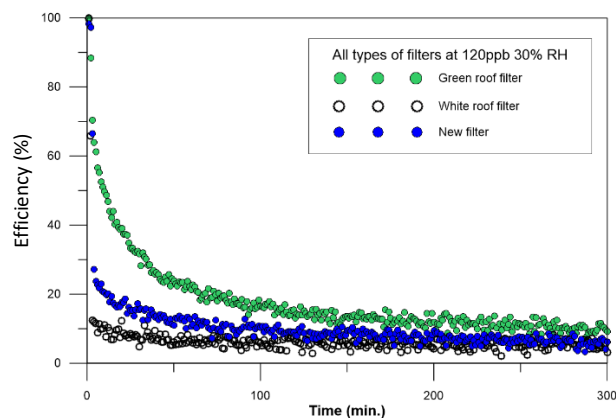
Figure 5 shows the ozone removal efficiency for tests conducted at two inlet ozone values, 40 and 120 ppb, and two relative humidity levels, 30 and 70%. Ozone removal efficiency is high at beginning of tests, decaying to a value of around 10% for both unused and white membrane roof filters after 5 hours of testing. For green roof filter tests, ozone removal efficiency have higher values than white membrane roof and unused filters for the first 150 mins, then the curve decays approaching a removal efficiency of 10% at the end of test. This decay behavior is also reported by Zhao (2007) and Hyttinen (2006) for both clean and deposit-loaded filters. Figures 5c and 5d show ozone removal efficiency for 40 ppb ozone inlet tests. The figures show similar trend of higher ozone removal at the start of tests. However, higher removal efficiency after 5 hours of testing are noticeable in comparison to 120 ppb tests.

To facilitate the comparison of ozone removal efficiency values, the average of the last 20 minutes of ozone removal efficiency of all tests are graphed together and shown in Figure 6.

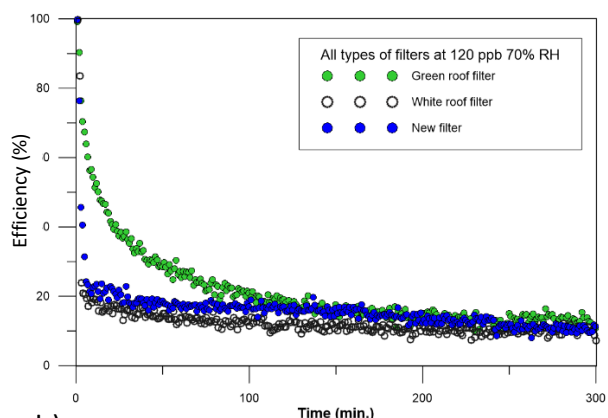
The figure shows that for all cases, ozone removal efficiency at 40 ppb inlet ozone is higher than the tests with 120 ppb, especially for green roof filters. This behavior may be a result of higher inlet ozone concentrations causing more rapid exhaustion of surface ozone reaction sites. The back-diffusion of new ozone reaction sites to the surface would be more competitive with consumption of sites at inlet O₃ levels of 40 ppb than at 120 ppb. The green roof filters tested generally had higher ozone removal efficiency than either filters taken from white or green rooftops. While reduced O₃ levels in ventilation air are, in isolation, beneficial, previous research indicates that volatile byproducts of ozone interacting with organic compounds from vegetation may be desorb from the filter and enter the airstream. This process may contribute to the degradation of perceived quality of ventilation air (Bekö et al. 2007b). Further research is necessary to characterize the volatile byproducts emitted from ozone chemistry on filters in service in HVAC systems on rooftops with green vs. white roof surfaces.

Figure 7 illustrates the relative humidity effect on ozone removal efficiency for both 40 and 120 ppb ozone inlet and for both 30 and 70% relative humidity tests. The subfigures show that the change in relative humidity has a minor effect on ozone removal for 40 ppb ozone inlet tests. However, a small increase in ozone removal efficiency is observed at 120 ppb ozone inlet with 70% relative humidity for the white membrane and unused filter tests, and less enhancement for the green roof filter tests. Shown in Figure 6 are bar graphs of ozone removal efficiencies after 5 hours with change in relative humidity. The differences in ozone removal efficiency at 30% RH and 70% RH at 40 ppb inlet ozone appears within the propagated uncertainty for all filters tested. At 120 ppb ozone inlet, the white membrane roof and unused filters show increased O₃ removal efficiency greater than the propagated uncertainty.

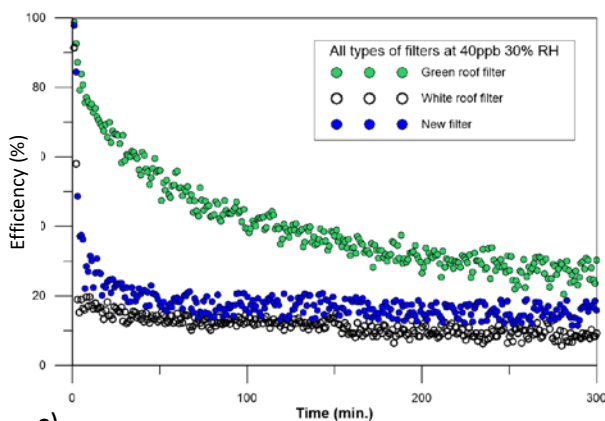
286



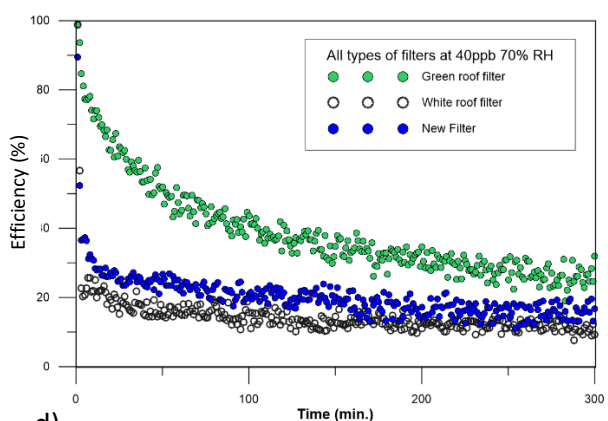
a)



b)



c)



d)

287

288 **Figure 5.** Ozone removal efficiency for green, white membrane, and unused (new) filter samples
 289 at 40, 120ppb, and 30, 70% relative humidity.

290

291

292 **Figure 6.** Ozone removal efficiency for green (GR), white membrane (WM) roofs, and new
293 (unused) filters at 40, 120ppb inlet ozone after 5 hours of testing. Low_RH=30%RH,
294 HighRH=70%RH. The values are the average of last 20 min. of each test. Error bars represent
295 the uncertainty as determined from an error propagation using instrument uncertainties.

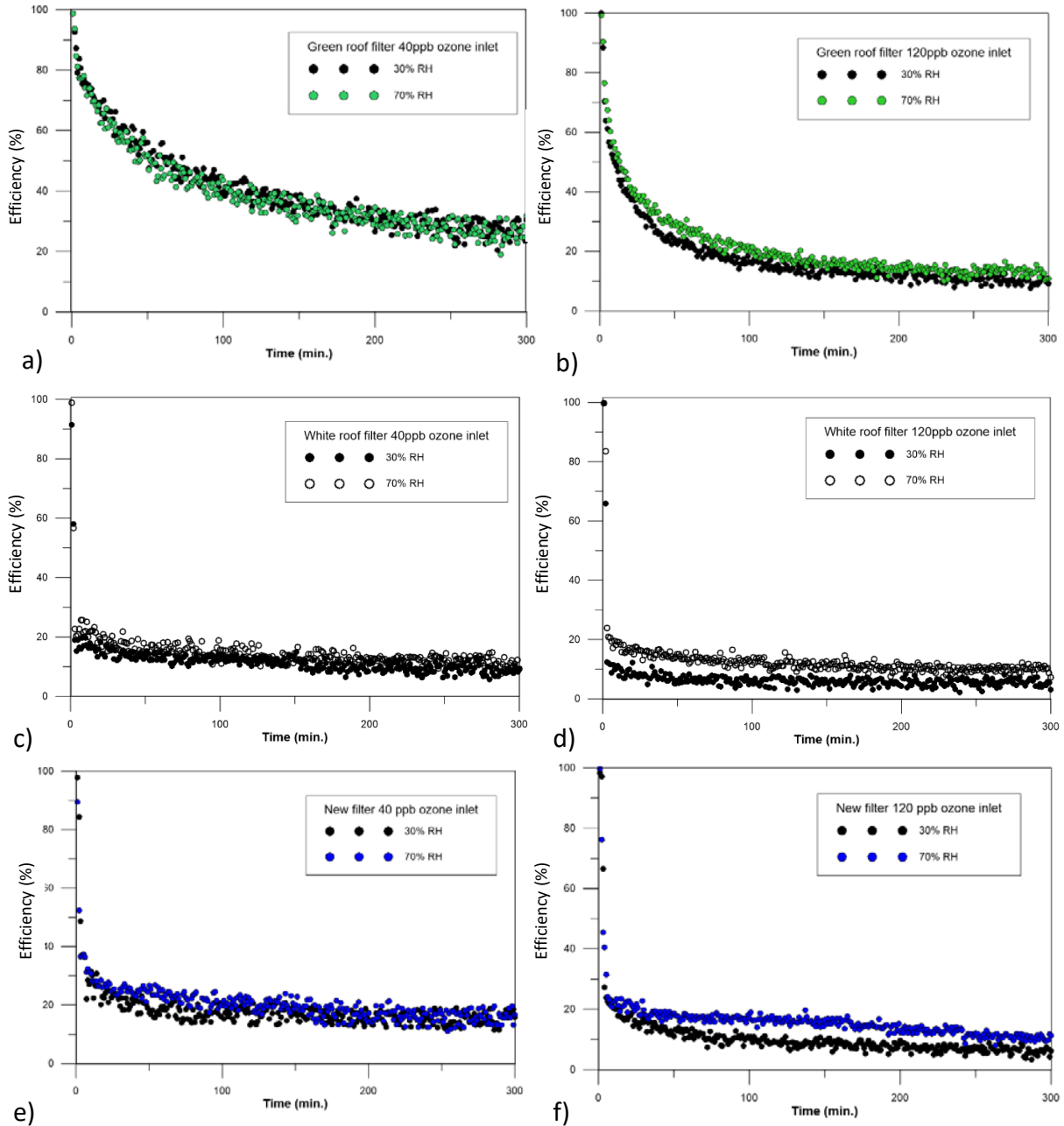


Figure 7. Relative humidity effect on ozone removal efficiency for green (panel a, b), white membrane roof (c,d), and unused filters samples (e,f) at 40, 120ppb ozone inlet, and 30, 70% relative humidity.

3.3 SEM IMAGES AND SURFACE ELEMENTAL ANALYSIS

Figure 8 shows SEM images for the green roof non-ozonated filter at low and high magnification. The figure shows high accumulation of deposits on filter fibers. A higher

magnification at 5000x in Figure 8b shows pollen and other deposits of biotic origin. These deposits are likely the predominant material causing higher ozone removal efficiency for green roof filters than other tested filters. Images of white membrane roof filter are shown in Figure 9. It is obvious that there are fewer deposits on the white membrane roof filter. However, some deposits are visible on the higher magnification image (Figure 9b). The lower level of deposits on this filter explains the lower ozone removal efficiency compared to green roof filter as ozone removal will depend mostly of the amount of particles accumulated and captured by filter fiber (Lin and Chen 2014). Figure 10 shows SEM images for unused filters. Figure 10a shows no deposits on the surface of fibers except in several location that could exist because of possible contamination during transportation, or sample preparation.

Figure 10b shows a furry fiber surface not evident in the white membrane roof fiber shown in Figure 9b. We hypothesize that the “furry” surface of the unused fibers have larger real surface area than fibers collected from filters servicing the white membrane roof; this difference in surface morphology may explain the reason behind higher ozone removal efficiency of unused filter samples in comparison with white membrane roof samples. The smoother surface observed in the fibers in filters taken from the white membrane roof could be attributed to exposure to air movement and moisture in the air stream passing through filters in air handling units

a) b)

Figure 8. SEM images for green roof filter samples non-ozonated at different magnification. a)100x. b) 5000x.

a) b)

Figure 9. SEM images for white membrane roof filter samples non-ozonated at different magnification. a)100x. b)5000x

a) b)

Figure 10. SEM images for unused filter samples non-ozonated at different magnification.
a)100x. b)5000x

To estimate and compare the composition of filter fibers and the deposits on fibers, an energy dispersive spectroscopy (EDS) elemental analysis was performed for locations on filter fibers and deposits shown in Figure 11 (yellow circles). The figure shows that measurements in at least two locations are performed for every filter type. Figure 12 show samples of EDS elemental analysis graphs for one location from each filter type. The average of numerical data of results for locations of interest in every filter are listed in Table 2.

351 a) b)

352

353

354

355

356

357 c) d)

358

359

360

361

362

363 e) f)

364 **Figure 11.** SEM images show locations (yellow circles) where elemental analysis was performed.
365 a) Non-ozonated unused filter fiber. b) Ozonated unused filter fiber. c) Non-Ozonated white
366 membrane roof filter fiber. d) Ozonated white membrane roof filter fiber and deposits. e) Non-
367 ozonated green roof fiber. f) Ozonated green roof fiber and deposits.

368

369 Figure 12a shows the analysis of a non-ozonated unused filter fiber. It reveals that carbon
370 and oxygen are the only compounds detected in the unused filter fiber. The average of duplicate
371 measurements in Table 2 show that carbon accounts for about 96% of the unused filter fiber
372 compounds, and oxygen accounts for the remaining 4%. This result is expected as the fiber
373 material is made of organic material comprising these two elements. For ozonated unused filter

fiber, the data in Table 2 shows a similar composition. However, there is a slight increase in oxygen percentage by about 1%. This increase may result from oxidization of filter fiber material resulting from exposure to ozone. Studies that demonstrate oxidation processes on filters with carbon-containing compounds results in formation of oxygen-containing surface functional groups support this concept (Lee and Davidson 1999).

Figure 12b shows elemental analysis of white membrane roof filter fiber. The figure and data in Table 2 show similar composition to unused filter fiber as the elements detected are carbon and oxygen only. For ozonated white membrane filter fiber, no meaningful difference in composition is seen from the unozonated white membrane roof filter, as shown in Table 2.

Figure 12c shows the analysis of a fiber of non-ozonated green roof filter. Note that EDS analysis for the filter fiber is different from that of the new and white membrane roof filter in that the fibers from the green roof filters were covered with deposits such that the EDS analyzer likely could not identify the fiber alone. We hypothesize this explains the similarity between non-ozonated new and white membrane roof filters and why the green roof filter fibers were substantially different in elemental composition. The figure and data in Table 2 show other elements present in green roof filters in addition to carbon and oxygen including silicon, iron, calcium, aluminum and other elements. These compounds are not detected on the fiber surfaces of unused and white membrane roof filters. The existence of these compounds may be attributed to deposits of on the filter fiber derived from vegetation, as shown in Figures 8b and 11f.

To obtain information about the elemental composition of large deposits on filter fibers, the data for deposits on both ozonated white membrane and ozonated green roofs is shown in Figures 11d and 11f are shown in Table 2. The data show that in addition to carbon and oxygen, silicon and iron form the highest percentage of elements, in addition to lower values of other

397 elements, in white membrane roof deposits. Existence of these elements may help to conclude
398 that these deposits are inorganic compounds (Hytinen et. al. 2006) that could originate from
399 soil-derived particles. For green roof filter deposits, the data show higher oxygen, silicon and
400 iron than deposits on white membrane roof.

401

402

403

404

405

406

407

408

409 a)

b)

410

411

412

413

414

415 c)

416 **Figure 12.** EDS elemental analysis graphs of filter fibers and deposits. a) Non-ozonated unused
417 filter fiber. b) Non-ozonated white membrane filter fiber. c) Non-ozonated green roof filter fiber.
418 Axes represent as following: Cps/Ev: counts per second per electron-volt, keV: kilo-electron-
419 volt.

420

421

Table 2. Elemental analysis data in normalized weight percent for different filter fibers and deposits gained using EDS analyzer. The values in table are the average of two locations of interest except where stated otherwise.

Specimen type	C	O	Na	Mg	Al	Si	P	S	Cl	K	Ca	Ti	Fe	Total
Non-ozonated new filter fiber	97.86	2.13	0	0	0	0	0	0	0	0	0	0	0	100
Ozonated new filter fiber	96.81	3.15	0	0	0.04	0	0	0	0	0	0	0	0	100
Non-ozonated WM roof fiber	98.27	1.72	0	0	0	0	0	0	0	0	0	0	0	100
Ozonated WM roof fiber	98.39	1.58	0	0	0	0	0	0	0	0	0	0	0	100
Non-ozonated GR filter fiber	74.12	14.06	0.47	0.24	1.06	3.73	0.08	0.26	0.31	0.51	1.39	0.24	3.57	100
Ozonated GR filter fiber	69.77	15.66	0.65	0.32	1.45	4.77	0.09	0.29	0.38	0.61	1.8	0.23	3.96	100
Ozonated deposits on WM filter ^{&}	88.08	7.16	0.29	0.06	0.88	1.98	0.03	0.01	0	0.06	0.25	0.04	1.16	100
Ozonated deposits on GR filter [%]	55.30	19.59	0.73	0.31	1.99	7.88	0.12	0.26	0.35	0.93	1.64	0.26	10.47	100

[&] Data represents the average of three location

[%] Data represents the average of four location

4. CONCLUSIONS:

In this study, ozone removal efficiency is determined from laboratory testing of filters from HVAC systems located on green roofs, white roofs, and for unused filters. The results show that the green roof filter exhibited greater ozone removal efficiency than the other filters, especially at the beginning of the tests. Ozone removal at the end of 5 hours (E_{5h}) showed ozone removal efficiency (for the 40 ppb test case) of about 26% for the green roof filter, white membrane and unused filters showed 10% and 15%, respectively. For the 120 ppb inlet ozone case, ozone removal efficiency is in the range of 5% to 15%. Test cases with higher relative humidity resulted in only a modest effect on ozone removal of the green roof filter, but ~5% increase for the white membrane roof and unused filters. These results indicate potential for rooftop surfaces to impact O_3 removal across filters. Future studies could investigate this phenomenon across more roofs with replicate samples to confirm these findings.

Scanning electron microscopy images show large deposits on the green roof filter that appear to contribute to the observed higher ozone reactivity. The images also show that unused

filter fibers have fuzzier surfaces than white membrane filter fibers. We hypothesize that this leads to greater surface area than that of the white roof used filter and therefore, higher ozone removal. Future work should consider nitrogen porosimetry analysis to measure fiber surface area to evaluate this hypothesis. Elemental analysis shows that the unused and white membrane roof filter fibers are mostly composed of carbon and oxygen, whereas the green roof filter surface contains other elements not present in the unused filter. This research demonstrates that HVAC filters installed in equipment on green roofs have a higher capacity to remove ozone. However, to better understand the role of green roof filters, additional measurements should be conducted, including measurement of VOC emissions from ozone chemistry occurring on loaded filters taken from rooftop HVAC systems.

Acknowledgments

The authors wish to acknowledge assistance from Don Mosely and Robin Morse of Walmart who provided access to the study site roof under support from a Walmart Realty Compliance Grant. The authors would also like to thank Wentai Luo, and Tom Bennett, of Portland State University for providing useful notes in the construction of the test rig, and Greg Baty for support in electron microscope center. Omed Abbass acknowledges the support of a scholarship from the Higher Committee of Education Development in Iraq (HCED). Elliott Gall was supported by the National Science Foundation under Grant No. 1605843. This research was supported in part by Assistance Agreement No. 83575401 awarded by the U.S. Environmental Protection Agency. It has not been formally reviewed by EPA. The views expressed in this document are solely those of the authors and do not necessarily reflect those of the Agency. EPA does not endorse any products or commercial services mentioned in this publication.

References

- Abbass, O.A., Sailor, D.J., Gall, E.T. (2017). Effect of fiber material on ozone removal and carbonyl production from carpets, *Atmospheric Environment*. 148, 42–48. doi:10.1016/j.atmosenv.2016.10.034.
- Bekö, G., Clausen, G., & Weschler, C. J. (2007a). Further studies of oxidation processes on filter surfaces: Evidence for oxidation products and the influence of time in service. *Atmospheric Environment*, 41(25), 5202-5212.
- Bekö, G., Clausen, G., & Weschler, C. J. (2007b). Sensory pollution from bag filters, carbon filters and combinations, *Indoor Air*, 18 (2008) 27–36. doi:10.1111/j.1600-0668.2007.00501.x.
- Berardi, U., GhaffarianHoseini, A., & GhaffarianHoseini, A. (2014). State-of-the-art analysis of the environmental benefits of green roofs. *Applied Energy*, 115, 411-428.
- Carslaw, N., Ashmore, M., Terry, A.C., Carslaw, D.C. (2015). Crucial Role for Outdoor Chemistry in Ultrafine Particle Formation in Modern Office Buildings, *Environ. Sci. Technol.* 49, 11011–11018. doi:10.1021/acs.est.5b02241.
- Coutts, A.M., Daly, E., Beringer, J., Tapper N.J. (2013). Assessing practical measures to reduce urban heat: Green and cool roofs, *Building and Environment*, 70, 266–276. doi:10.1016/j.buildenv.2013.08.021.
- Davis, J. M., & Speckman, P. (1999). A model for predicting maximum and 8h average ozone in Houston. *Atmospheric Environment*, 33(16), 2487-2500.
- De Smedt, F., De Gendt, S., Heyns, M. M., & Vinckier, C. (2001, January). Materials compatibility and organic build-up during ozone-based cleaning of semiconductor devices. In *DIFFUSION AND DEFECT DATA PART B SOLID STATE PHENOMENA* (pp. 63-66). Scitec Publications; 1999.
- Destailats, H., Chen, W., Apte, M. G., Li, N., Spears, M., Almosni, J., ... & Fisk, W. J. (2011). Secondary pollutants from ozone reactions with ventilation filters and degradation of filter media additives. *Atmospheric environment*, 45(21), 3561-3568.
- EPA, 2015. NAAQS Table. An online content from U.S. Environmental Protection Agency website. <https://www.epa.gov/criteria-air-pollutants/naaqs-table>. Reached on Dec. 2016.
- Gryparis, A., Forsberg, B., Katsouyanni, K., Analitis, A., Touloumi, G., Schwartz, J., ... & Wichmann, H. E. (2004). Acute effects of ozone on mortality from the “air pollution and health: A European approach” project. *American journal of respiratory and critical care medicine*, 170(10), 1080-1087.
- Hyttinen, M., Pasanen, P., & Kalliokoski, P. (2006). Removal of ozone on clean, dusty and sooty supply air filters. *Atmospheric Environment*, 40(2), 315-325.
- Lai, D., Karava, P., Chen, Q. (2015). Study of outdoor ozone penetration into buildings through ventilation and infiltration, *Building and Environment*, 93, 112–118. doi:10.1016/j.buildenv.2015.06.015.

504 Lee, P., & Davidson, J. (1999). Evaluation of activated carbon filters for removal of ozone at the
 505 ppb level. *American Industrial Hygiene Association Journal*, 60(5), 589-600.

506 Lin, C. C., & Chen, H. Y. (2014). Impact of HVAC filter on indoor air quality in terms of ozone
 507 removal and carbonyls generation. *Atmospheric Environment*, 89, 29-34

508 Lippmann, M. (1989). Health effects of ozone a critical review. *Japca*, 39(5), 672-695.
 509 <http://dx.doi.org/10.1080/08940630.1989.10466554>

510 Massey, D., Kulshrestha, A., Masih, J., Taneja, A. (2012). Seasonal trends of PM10, PM5.0,
 511 PM2.5 & PM1.0 in indoor and outdoor environments of residential homes located in North-
 512 Central India, *Building and Environment*, 47, 223–231. doi:10.1016/j.buildenv.2011.07.018.

513 Morrison, G. C., Nazaroff, W. W., Cano-Ruiz, J. A., Hodgson, A. T., & Modera, M. P. (1998).
 514 Indoor air quality impacts of ventilation ducts: ozone removal and emissions of volatile organic
 515 compounds. *Journal of the Air & Waste Management Association*, 48(10), 941-952.

516 Oleson, K. W., Bonan, G. B., & Feddema, J. (2010). Effects of white roofs on urban temperature
 517 in a global climate model. *Geophysical Research Letters*, 37(3).

518 Pudasainee, D., Sapkota, B., Shrestha, M. L., Kaga, A., Kondo, A., & Inoue, Y. (2006). Ground
 519 level ozone concentrations and its association with NOx and meteorological parameters in
 520 Kathmandu valley, Nepal. *Atmospheric environment*, 40(40), 8081-8087.

521 Rim, D., Gall, E.T., Maddalena, R.L., Nazaroff, W.W. (2016) Ozone reaction with interior
 522 building materials: Influence of diurnal ozone variation, temperature and humidity, *Atmospheric*
 523 *Environment*, 125, 15–23. doi:10.1016/j.atmosenv.2015.10.093.

524 Sailor, D. J. (2008). A green roof model for building energy simulation programs. *Energy and*
 525 *buildings*, 40(8), 1466-1478.

526 Sailor, D. J., Elley, T. B., & Gibson, M. (2012). Exploring the building energy impacts of green
 527 roof design decisions—a modeling study of buildings in four distinct climates. *Journal of Building*
 528 *Physics*, 35(4), 372-391.

529 Shao, M., Lu, S., Liu, Y., Xie, X., Chang, C., Huang, S., & Chen, Z. (2009). Volatile organic
 530 compounds measured in summer in Beijing and their role in ground-level ozone formation.
 531 *Journal of Geophysical Research: Atmospheres*, 114(D2).

532 Shields, H. C., Weschler, C. J., & Naik, D. V. (1999). Ozone removal by charcoal filters after
 533 continuous extensive use (5 to 8 years). *Indoor Air*, 99, 49-54.

534 Stephens, B., Gall, E. T., & Siegel, J. A. (2011). Measuring the penetration of ambient ozone
 535 into residential buildings. *Environmental science & technology*, 46(2), 929-936.

536 Taha, H., & Sailor, D. (2010). Evaluating the Effects of Radiative Forcing Feedback in
 537 Modelling Urban Ozone Air Quality in Portland, Oregon: Two-Way Coupled MM5–CMAQ
 538 Numerical Model Simulations. *Boundary-layer meteorology*, 137(2), 291-305. Doi:
 539 10.1007/s10546-010-9533-9

540 Weschler, C. J., Shields, H. C., & Naik, D. V. (1994). Ozone-removal efficiencies of activated
541 carbon filters after more than three years of continuous service. *ASHRAE transactions*, 100(2),
542 1121-1129.

543 Yang, S., Zhu, Z., Wei, F., Yang X. (2017). Carbon nanotubes / activated carbon fiber based air
544 filter media for simultaneous removal of particulate matter and ozone, *Building and*
545 *Environment*, 125, 60–66. doi:10.1016/j.buildenv.2017.08.040.

546 Zaatari, M., Novoselac, A., Siegel J. (2014). The relationship between filter pressure drop,
547 indoor air quality, and energy consumption in rooftop HVAC units, *Building and Environment*,
548 73, 151–161. doi:10.1016/j.buildenv.2013.12.010.

549 Zhao, P., Siegel, J. A., & Corsi, R. L. (2007). Ozone removal by HVAC filters. *Atmospheric*
550 *Environment*, 41(15), 3151-3160.

551